RESEARCH ARTICLE | OPEN ACCESS

Eoldist, a Web Application for Estimating Cautionary Detection Distance of Birds by Automatic Detection Systems to Reduce Collisions With Wind Turbines

Julie Fluhr[1] | Olivier Duriez[1] | Constance Blary[1,2] | Thierry Chambert[1] | Bettina Almasi[3] | Patrik Byholm[4,5] | Nelleke H. Buitendijk[6] | Jocelyn Champagnon[7] | Mindaugas Dagys[8] | Wolfgang Fiedler[9] | Charlotte Francesiaz[10] | Frédéric Jiguet[11] | Simon Lee[12,13] | Alexandre Millon[14] | Flavio Monti[15] | Lucile Morcelet[14] | Ran Nathan[16] | Bart A. Nolet[6,17] | Rascha Nuijten[6] | Philippe Pilard[18] | Cécile Ponchon[19] | Alexandre Roulin[20] | Carlos D. Santos[9,21] | Orr Spiegel[22] | Kim Schalcher[20] | Aurélie De Seynes[23] | Geert Spanoghe[24] | Martin Wikelski[9] | Ramunas Žydelis[25] | Aurélien Besnard[26]

[1]CEFE, Univ Montpellier, CNRS, EPHE, IRD, Montpellier, France | [2]CEFE, ADEME, Angers, France | [3]Swiss Ornithological Institute, Sempach, Switzerland | [4]Novia University of Applied Sciences, Ekenäs, Finland | [5]Organismal & Evolutionary Biology, University of Helsinki, Helsinki, Finland | [6]Department of Animal Ecology, Netherlands Institute of Ecology, Wageningen, The Netherlands | [7]Tour du Valat, Research Institute for Conservation of Mediterranean Wetlands, Arles, France | [8]Nature Research Centre, Vilnius, Lithuania | [9]Max Planck Institute of Animal Behavior, Radolfzell, Germany | [10]Office Français pour la Biodiversité, Direction Recherche et Appui Scientifique, Juvignac, France | [11]CESCO, MNHN CNRS Sorbonne Université, Paris, France | [12]Centre for Ecology and Conservation, University of Exeter, Penryn, UK | [13]Natural England, Sterling House, Dix's Field, Exeter, UK | [14]Aix Marseille Univ, Avignon Univ, CNRS, IRD, Institut Méditerranéen Biodiversité & Ecologie (IMBE), Aix-en-Provence, France | [15]Institute of Research on Terrestrial Ecosystems (IRET), National Research Council (CNR), Lecce, Italy | [16]Hebrew University of Jerusalem, Jerusalem, Israel | [17]Department of Theoretical and Computational Ecology, Institute for Biodiversity and Ecosystem Dynamics, University of Amsterdam, Amsterdam, The Netherlands | [18]LPO, Arles, France | [19]CEN PACA, Saint-Martin-de-Crau, France | [20]Lausanne University, Lausanne, Switzerland | [21]MARE - Marine and Environmental Science Centre and ARNET - Aquatic Research Network Associate Laboratory, Department of Environmental Sciences and Engineering, NOVA School of Science and Technology, NOVA University Lisbon, Caparica, Portugal | [22]School of Zoology, Faculty of Life Sciences, Tel Aviv University, Tel Aviv, Israel | [23]LPO, Campan, France | [24]Research Institute for Nature and Forest, Brussels, Belgium | [25]Ornitela, UAB, Vilnius, Lithuania | [26]CEFE, Univ Montpellier, CNRS, EPHE-PSL University, IRD, Montpellier, France

Correspondence: Olivier Duriez (olivier.duriez@cefe.cnrs.fr)

ABSTRACT

The installation of automatic detection systems (ADSs) on operating wind energy facilities is a mitigation measure to reduce bird collisions. The effectiveness of an ADS depends on a combination of parameters, including the detection distance of the bird, its flight speed, and the time to complete the chosen action (e.g., turbine shutdown). We created a web application, *Eoldist*, to calculate cautionary detection distances required by an ADS, using bird flight speed and turbine shutdown time as input parameters. We compiled a database of the flight speeds of 168 Western Palearctic birds from a review of scientific literature supplemented by an analysis of unpublished GPS-tracking datasets. To estimate turbine shutdown time, we

---

Julie Fluhr and Olivier Duriez contributed equally to the writing of the paper.

1 | Introduction

A crucial requirement for the energy transition is the development of renewable energies such as wind power [1]. However, this emerging infrastructure can have negative impacts on biodiversity [2]. One impact is the loss of natural habitats; for example, frightened or disturbed animals can avoid infrastructure sites [3, 4]. Another is that flying animals such as birds and bats often collide with wind turbine blades or towers [5–7]. These impacts may ultimately threaten the viability of affected populations [8], a concern that is growing with the sharp rise in the number of wind energy facilities (hereafter WEFs) worldwide [9–11]. This makes it urgent to find solutions to reduce negative impacts and ensure that the wind industry develops in a way that minimizes harm to biodiversity.

To reduce the risk of collision, WEF operators can install an automatic detection system (ADS) near or on a turbine mast. An ADS operates through the remote detection and identification of "bird targets." Different types of technology are used to detect birds, including radar or optical (including thermal) cameras, sometimes used in combination [12, 13]. Large birds (or flocks) can be detected at distances up to 8 km with radar ADS, but with optical ADS, detection distances rarely exceed 1 km for large birds such as eagles and around 600 m for smaller species [12, 13]. Once a target has been detected, identified, and its trajectory analyzed by the ADS [14, 15], several types of actions can be triggered: a scare signal (usually auditory) to prompt individuals to change their trajectory and move away from a turbine, the slowing down or stopping of the turbines to minimize the risk of collision, or doing nothing. Yet ADS effectiveness in reducing collisions has rarely been scientifically investigated, a notable exception being a study of a specific type of ADS in North America [16]. Field evidence has shown that at some WEF, significant numbers of collisions still occur even after an ADS has been installed on every turbine (e.g., [8, 17]), and very few studies rigorously quantified the reduction in collision rate [18]. The reasons why an ADS fails to prevent some collisions are not well known and are likely to be multifactorial: (1) technical problems, such as failure of the ADS, problems in the transmission of orders between the ADS and the turbine, and (2) methodological problems, such as difficulties of detection or classification by the ADS (related to the type of bird, the physical surroundings—such as topography and vegetation—the orientation of the sun, the weather) that delay the detection of birds, and the too slow deceleration of turbines. Therefore,

in some situations, an ADS simply cannot prevent a collision because it does not trigger a reaction fast enough.

The effectiveness of an ADS is inherently based on a combination of the detection distance of a bird, its flight speed and trajectory, and the time taken to complete the chosen action (emitting a scare signal or shutting down the turbine). In this study, we focused on turbine shutdown. As a precautionary principle, we chose the hypothesis of a worst-case scenario of a bird flying at constant speed in a straight line towards the wind turbine (as changes in direction would induce a delay in arriving at the turbine, hence increasing time required to stop the turbine and decreasing detection distance). In this case, we define the cautionary detection distance D as provided in Equation (1):

$$D = \left[T_{shutdown} * V_{bird} \right] + L_{blade} \tag{1}$$

where D varies according to bird flight speed V_{bird}, turbine blade length L_{blade}, and the total time to shutdown $T_{shutdown}$ [19]. Note that we assumed that birds can arrive from all directions towards the turbine, and we included turbine blade length in Equation (1) in order to define the radius of the sphere where collisions may occur; hence, this radius must be added to the detection distance. The parameter $T_{shutdown}$ is the sum of three components: the time of the ADS to detect and classify a bird target $T_{decision}$, the time to send the shutdown order to the wind turbine control center (Supervisory Control and Data Acquisition [SCADA] system) T_{signal}, and the time to slow the turbines T_{brake} to a speed that is no longer a risk for the bird. For example, if a bird is detected at a distance of 200 m and is flying at 20 m s^{-1}, it will cover the distance to the turbine in 10 s if it follows a direct linear trajectory to the turbine. If it is detected at 400 m, it will cover this distance in 20 s, thus doubling the time available to slow down/stop the blades. However, if the blade deceleration time is 30 s, the bird would need to be detected at 600 m to effectively prevent the collision. This means that there may be situations when the collision risk cannot be fully reduced because (i) the bird flies too fast and/or (ii) the turbine shutdown is too slow. In such cases, even the most sophisticated ADS would be useless if it was unable to detect the bird at a sufficient distance. It is thus of prime importance for ADS stakeholders to have accurate information about the required detection distance for relevant bird species in order to trigger a reaction in time. So, our objective was to highlight the necessity to consider these two components (bird speed and shutdown time) and the resulting cautionary detection distance before investing in a costly ADS.

In Equation ([1]), the source of the variability of D is related to L_{blade}, $T_{shutdown}$, and bird flight speed V_{bird}. Turbine deceleration time T_{brake} has rarely been studied, but we hypothesized that it is likely to depend on (i) initial rotation speed (which depends directly on wind speed in synchronous turbines or indirectly in asynchronous wind turbines), (ii) blade length (long blades have more inertia than short blades), and (iii) pitch rate of the blade (which spins the blades in the opposite direction of the wind to initiate a braking effect).

In contrast, bird flight speeds have been widely studied and are known to be affected by several factors. They depend on (1) bird morphology (including wingspan, wing area, body mass, wing loading—that is, the ratio between the last two parameters—and wing shape) [20–22]; (2) type of flight (flapping, gliding, soaring, hovering, and the proportion of these in a bird's flight patterns, which varies between species) [23]; (3) environmental conditions (including mainly wind speed and direction, which also affect D through its effect on $T_{shutdown}$, as well as altitude, which affects air density) [24–26]; and (4) flight context (the speed during local flights may be different from that in migratory flights because the bird's needs and motivation are different) [27]. An overview of factors affecting bird flight speeds is provided in ESM 01. Given the many factors influencing a bird's flight speed, there is great variability between species, between individuals within a species, and according to the seasonal context. This makes it very important to consider the range of possible flight speeds for a given species when studying the ideal detection distance to reduce its risk of collision with turbines.

The goal of this study was to objectively assess the detection distance needed for an ADS to react in time, providing robust, reliable, and useable information for stakeholders to make relevant decisions. Based on data from a variety of sources and collected in the field, we developed a web application (*Eoldist*, an acronym combining the French word "éolienne" (wind turbine) and "distance") that calculates detection distances for specific turbine characteristics and bird species. The focus was on onshore WEF and thus on terrestrial bird species. To this end, we compiled a database of flight speed ranges for 168 species (from all orders of Western Palearctic avifauna) through a search of published literature, supplemented with analyses of tracking data from partners, or computed theoretical flight speeds derived from aerodynamic theory [22]. We estimated turbine shutdown time $T_{shutdown}$ by conducting field experiments at seven WEF. This allowed us to identify the parameters driving shutdown time, including blade length, type of machine (synchronous vs. asynchronous), and wind speed. After developing the application, we tested it on calculations for a set of bird species to analyze the effect of different parameters on cautionary detection distance D.

2 | Methods

To estimate cautionary detection distance D (see Equation [1] in Section [1]), it is necessary to get an accurate distribution of bird flight speed V_{bird} and an estimate of turbine shutdown time $T_{shutdown}$.

2.1 | Bird Flight Speed (V_{bird})

2.1.1 | Flight Speed Measurement Methods

Most studies about bird flight (e.g., [20]) report "airspeed" values, that is, the relative speed at which the bird is moving through the air mass (also called "relative wind," with the bird in flight as the reference). Airspeed is actually the most important factor for aerodynamics computing [22]. However, for the purpose of determining cautionary detection distances for birds approaching wind turbines, the reference point for estimating bird speed must not be the bird in the air flow but rather be the turbine, that is, a fixed point on the ground. The bird flight speed relative to a fixed point on the ground is called "groundspeed." Therefore, using groundspeed makes more sense in the context of an obstacle fixed on the ground, such as a wind turbine, while for collisions with aircraft moving in the same airflow as birds, airspeed would be better suited. Depending on the availability of bird speed data for a given species, we preferentially used groundspeed values where available, and secondarily, airspeed (assuming that in the absence of wind, airspeed and groundspeed are identical and that bird speeds have chances to be recorded both in tailwind and in headwind).

There are three main tools to estimate the flight speed of tracked birds. One of these, radar, can be used to track bird movements day and night; it has mainly been used during migratory periods [28–30]. Another is an instrument called an ornithodolite, which combines binoculars with a laser rangefinder, inclinometer, and digital magnetic compass; it can record the positions of a bird in flight in a 3D space in real time [31]. This portable tool has been used to measure the flight speeds of birds in local and migratory flights [32, 33]. Published data from both radar and ornithodolite are reported as airspeeds (actually measuring groundspeed but correcting for wind speed and direction a posteriori). Another tool is satellite telemetry, in which birds are tagged with miniature GPS receivers that record 3D geographical position at regular timestamps, as well as instantaneous groundspeed [34]. Satellite telemetry allows bird flight behavior to be recorded independently of the observer's position throughout the year, during local and migratory flights. In our study, data collected by all these tools (GPS telemetry, radar, or ornithodolite) was grouped under the category "observed" speeds.

Airspeeds can also be computed using aerodynamic theory using the Flight program [22], which can predict the flight speed of a species as a function of its mass, wingspan, and wing area. For species that use flapping flight, it is possible to predict the flight speed that allows the bird to expend the least energy per unit of time (V_{mp}, or "minimal power speed") and the speed that allows it to cover the largest distance travelled per energy expended (V_{mr}, or "maximum range speed"). For gliding species, it is also possible to predict the flight speed that minimizes the bird's loss of altitude per unit of distance travelled (V_{bg}, or "best glide speed"). Gliding birds can also use an "optimal speed" (V_{opt}) that maximizes cross-country speed by adjusting the gliding speed to the rate of ascent during soaring phases [22, 35]. In their local movements, birds generally fly at speeds close to or slightly above V_{mp} (V_{bg} for

soaring/gliding species), while they generally choose V_{mr} (V_{opt} for soaring/gliding species) when they need to maximize the distance travelled during long migratory flights [36]. Flight speeds estimated using aerodynamic computing are airspeed and are referred to as "theoretical" flight speeds in the *Eoldist* application.

2.1.2 | Flight Speed Data

To build the flight speed database, our aim was to collect flight speed values for at least one species for each of the 27 orders of birds present in the Western Palearctic. As a first step, we used the Web of Science and the Google Scholar search engines with the following keywords: speed*, bird*, avian, flight. In a second step, we used the Movebank database (http://www.movebank.org) to search for any species missing after our literature review. We then asked data owners to share GPS-tracking data for additional species or periods for flight speeds not found in publications. We analyzed tracking data by distinguishing contexts of migratory and local movement (see ESM 02). We defined "migration" as medium- to long-distance movements, including migratory and dispersal flights in juvenile individuals, and "local" as short-distance movements such as foraging flights, transits between a feeding area and the colony, and courtship or hunting flights. In a third step, for species with no published data or no GPS-tracking data, we computed theoretical flight speed using the Flight program [22].

We used instantaneous groundspeed (i.e., measured directly by the GPS tag or radar at short time intervals of 1–3 s), while values of speed averaged between subsequent intervals (typically > 1 min intervals) were discarded because of possible bias [25]. Average migration speeds, generally recorded at intervals of several minutes, hours, or days, are unsuitable to describe the range of groundspeeds required for the purpose of this study [37].

As flight groundspeed can be highly variable (see ESM 01), our goal was not to provide a single estimate of average flight speed but a frequency distribution of flight speeds reflecting heterogeneity in conditions and among conspecifics. For this purpose, we retrieved mean flight speed ($\pm$SD) from the literature or our data analysis. To get an average flight speed value when several estimates were available from the literature, *EolDist* uses the following procedure: (1) an overall (empirical) distribution is generated using a parametric bootstrap based on the distribution (point estimate$\pm$confidence interval) of each estimate from the literature (assuming a normal distribution); (2) the average of that empirical distribution is then reported as the average flight speed value. Because theoretical calculations of flight (air)speed are not associated with a SD, we applied a generic coefficient of variation (CV) that corresponded to the average CV estimated from species tracked by GPS or radar.

2.2 | Turbine Shutdown Time ($T_{shutdown}$)

To shut down a turbine, an ADS triggers the blades to spin against the wind (pitch rate), resulting in slow, smooth braking.

The calculation in Equation (1) requires estimates for turbine shutdown time $T_{shutdown}$, data that is generally not available. Therefore, we conducted specific field experiments to measure this.

2.2.1 | Field Protocol

We designed a simple experimental protocol that volunteer WEF operators carried out in summer 2021 in France. Each operator involved in a field test had to record turbine rotation speed, then trigger a shutdown and record decelerating rotation speed, measured in rotations per minute (rpm) every 1 s or every 5 s, during 90 s. Experimenters recorded both the intrinsic parameters of the wind turbine and the environmental parameters likely to affect $T_{shutdown}$ (namely, the wind speed). The intrinsic parameters were blade length (L_{blade}), nacelle height, and type of turbine. Wind turbines are divided into two main types according to whether the architecture of their electrical generator is synchronous or asynchronous. A synchronous generator has a direct mechanical drive between the hub of the turbine and the generator. An asynchronous generator requires operation at a rated speed of several hundred revolutions per minute, which requires the use of a gearbox between the rotor and the generator. Data about pitch rate was not known by operators, so it was not recorded. The environmental parameters were the initial wind speed and direction, recorded continuously in the wind turbines. We requested that each experiment should be performed 10 times for each possible turbine model and for three wind classes (< 10, $10–20$, and $> 20\,\mathrm{m\,s^{-1}}$).

2.2.2 | Statistical Analysis

We hypothesized that the probability of turbine shutdown (i.e., decelerating below a certain threshold) before 90 s and $T_{shutdown}$ were likely to be influenced by the following variables: type of turbine (synchronous or asynchronous), height of the nacelle, length of the blades, initial wind speed (at the time of shutdown), and initial rotation speed of the rotor (measured in rpm). We performed analyses with uncorrelated variables only.

In a first step, we modelled the probability that the residual rotor speed reached a given threshold between the initiation of the rotor stop command by the turbine command center (SCADA) and the end of the test (t = 90 s) as a function of the explanatory variables selected from the correlation analysis (ESM 03). Two thresholds of residual rotor speed (3 and 2 rpm) were tested (consistent with discussions with WEF operators and environmental agencies).

In a second step, we estimated the time needed for the rotor to reach the residual rotation speed (conditional to the fact that this threshold had been reached during the 90 s of the test) from a linear model (LM) based on a normal distribution of the data and an identity link. This duration was modelled as a function of different explanatory variables tested separately, as well as additively and in interaction. The objective was to identify which variable(s) significantly influenced the rotor deceleration time

$T_{shutdown}$ and, if so, what percentage of the variance in the dataset they explained.

A backward stepwise model selection, based on the Akaike information criterion (AIC), allowed the best model to be selected for each residual rotation speed tested, in other words, to highlight the explanatory variable(s) that best described the variability in the dataset. We used the best model to predict values and the SD of $T_{shutdown}$ according to the input explanatory variables.

2.3 | Building the *Eoldist* Web Application

Using this data, we used the Shiny package in R Studio to develop an application that calculates the cautionary detection distance D using Equation (1). The application includes three sub-programs: one calculates a range of flight speeds for the referenced bird species, the second the turbine shutdown time according to different parameters related to the wind turbine, and the third the detection distance needed for that species. Graphically, the application is organized in two sections, one for each sub-program. Under each section, a left panel allows the user to choose the calculation parameters, and the results are represented graphically in the right panel (see Figure 1).

2.3.1 | Integration of Flight Speed

In the "Flight speed" sub-program, the user goes to "Enter bird data" in the left panel to select the bird species and flight context (migration or local flight) from the database of 168 species presented, which displays the mean ($\pm$ SD) flight speed of the species. The top right panel displays the probability distribution of flight speeds, that is, the range of possible flight speeds of the species in the flight context chosen by the user. This distribution was built from the observed or theoretical average flight speed values ($\pm$ SD) (as explained above) of the species in the chosen flight context using a normal distribution. When more than one type of data is available for a species, the observed speeds are prioritized over the theoretical speeds. The type(s) of data used (groundspeed for GPS recording, airspeeds for radar, ornithodolite, and theoretical computations) and the average speed ($\pm$ SD) of the species are displayed below the graph.

2.3.2 | Integration of Turbine Shutdown Time

While data is lacking about $T_{decision}$ and T_{signal}, after discussions with ADS manufacturers and WEF operators, we considered that the values for these parameters are generally extremely short. McClure, Martinson, and Allison [12] found a classification time of 0.2 s for one specific type of ADS (Identiflight). Hence, to be conservative, we set $T_{decision}$ and T_{signal} at 1 s each, and thus $T_{shutdown} = T_{brake} + 2$.

Using the data from our field tests for turbine shutdown time $T_{shutdown}$, the second sub-program allows the user to choose the values of the parameters used to compute the average turbine shutdown time $T_{shutdown}$ ($\pm$ SD) to reach a residual rotation speed. Under "Enter wind turbine data," the user enters the values of the four parameters on which $T_{shutdown}$ is modelled (see Section 3): (i) type of machine (type of turbine:synchronous or asynchronous); (ii) blade length (parameter used to model turbine deceleration time and also included in Equation (1); based on the data collected in the field protocol for WEF operators, the current range of possible values for blade length is between 35 and 56 m for synchronous machines, and between 40 and 63 m for asynchronous machines); (iii) mean initial wind speed (from an average wind speed of 5, 10, or 15 m s^{-1} on which the rotor deceleration time is modelled; see Section 3); and (iv) residual rotation speed (from 1, 2, or 3 rpm) to calculate the time required to reach this threshold (i.e., rotor speed equal to or lower than this threshold) once the stop command is issued. The formula for converting an angular velocity (N) expressed in rpm into a linear velocity (V) at the blade tip expressed in meters per second (m s^{-1}) is the following: $V = \frac{2\pi * r}{60} * N$ with r the blade length of the turbine.

The output of the second sub-program is the turbine shutdown time $T_{shutdown}$ (i.e., turbine deceleration duration) in seconds.

If the user has independently measured $T_{shutdown}$ at a particular WEF, we added the possibility to manually enter a value for $T_{shutdown}$ that by-passes the previous calculation based on turbine features and wind speed.

2.3.3 | Cautionary Detection Distance Sub-Program (D)

Using the parameters previously estimated (V_{bird} and $T_{shutdown}$), *Eoldist* then calculates the cautionary detection distance D for the species. This distance is displayed graphically in the bottom right panel as the cumulative distance D for the species in the chosen flight context (local or migration) according to the percentage of detected flights of the species. This percentage of detected flights is defined by the user with the slider above the graph. The higher the percentage of detected flights, the more accurate the range of possible flight speeds of the species (i.e., minimizing the right-tail of the frequency distribution of flight speeds). The user can vary the percentage of detected flights in 5% step increments.

2.4 | Examples of Cautionary Detection Distance D

2.4.1 | Effect of Type of Flight, Turbine Characteristics, Wind Speed, and Residual Rotation Speed

As a first example, we calculated D for a species highly impacted by collisions in our study area: the lesser kestrel (*Falco naumanni*). We used the parameters for a WEF in southern France at which all turbines are equipped with an ADS, yet collisions are still regularly recorded [8]. The WEF combines two types of asynchronous machines: one with a mast height of 56 m and blade length of 35 m, and a second with a mast height of 78 m and blade length of 41 m. We ran calculations for local flights and migratory flights, with two residual rotation speeds (3 and 2 rpm). All calculations were performed with an initial wind speed of 10 m s^{-1} and a flight detection threshold of 95%.

FIGURE 1 | Legend on next page.

FIGURE 1 | Screenshot of the *Eoldist* application, parameterized for a lesser kestrel (*Falco naumanni*) in local flight (top left panel) at a wind energy facility with asynchronous machines with 35-m blades, an initial wind speed of $10 \, \mathrm{m\,s^{-1}}$ and a residual rotation speed of 3 rpm (bottom left panel). The program first displays a frequency distribution of flight (ground)speeds for the species, calculated from source data (top right panel). Underneath this, the program calculates the estimated turbine shutdown time and displays the cumulative cautionary detection distance curve (bottom right panel). On this curve, a dotted line indicates the precise cautionary detection distance in relation to the percentage of detected flights (here 95% of detected flights results in a cautionary detection distance of 315 m).

In a second example, we studied the effect of initial wind speed, blade length, and type of machine on *D* for a lesser kestrel in local flight. We ran calculations for three initial wind speeds (5, 10, and $15 \, \mathrm{m\,s^{-1}}$) for synchronous machines with blade lengths between 35 and 50 m and for asynchronous machines with blade lengths between 45 and 60 m.

2.4.2 | Effect of Percentage of Detected Flights

In a third example, we studied the effect of the percentage of detected flights on *D*. We used two species of similar body mass (~10 kg) and similar average groundspeed, the Bewick's swan (*Cygnus columbianus bewickii*) and the griffon vulture (*Gyps fulvus*). Bewick's swans use only flapping flight, resulting in a groundspeed with little variance ($15.2 \pm 0.7 \, \mathrm{m\,s^{-1}}$), while griffon vultures are specialists of soaring/gliding flight, resulting in a groundspeed with large variation ($15.3 \pm 5.3 \, \mathrm{m\,s^{-1}}$). All calculations were computed for birds in local flights with an initial wind speed of $10 \, \mathrm{m\,s^{-1}}$ and for an asynchronous machine with a blade length of 45 m and a residual rotation speed of 3 rpm. We varied the percentage of flights detected between 25% and 95%.

2.4.3 | Effect of Blade Length and Shutdown Time for Protected Species

Finally, we investigated the effect of two parameters (residual rotation speed and $T_{shutdown}$) on *D* for 10 bird species of high conservation concern in France or Europe [38]: red-backed shrike (*Lanius collurio*), Montagu's harrier (*Circus pygargus*), red kite (*Milvus milvus*), common swift (*Apus apus*), black stork (*Ciconia nigra*), little bustard (*Tetrax tetrax*), white-tailed eagle (*Haliaeetus albicilla*), griffon vulture (*G. fulvus*), common snipe (*Gallinago gallinago*), and common eider (*Somateria mollissima*). These species were also selected as they represent a large gradient of sizes and masses (from the 30-g red-backed shrike to the 10-kg griffon vulture), as well as a large gradient of flight types (from the flapping flight of ducks and waders to specialists of gliding such as raptors) and of flight speeds (from the Montagu's harrier flying at an average $6.4 \, \mathrm{m\,s^{-1}}$ to the common eider at $18.5 \, \mathrm{m\,s^{-1}}$). We performed calculations for these species with two asynchronous wind turbine models: one with a blade length of 45 m (typical of current turbines), and one with a blade length of 63 m (the largest blade length available, expected to be commonly used in the coming years for repowering WEF). We used two thresholds of decelerating rotation speed: 3 rpm for the 45-m blades (corresponding to a linear speed of $51 \, \mathrm{km\,h^{-1}}$ at blade tip) and 2 rpm for the 63-m blades (corresponding to a similar linear speed of $50 \, \mathrm{km\,h^{-1}}$ at blade tip). All calculations were computed for birds in local flights, with an initial wind speed of $10 \, \mathrm{m\,s^{-1}}$ and 95% of flights detected.

3 | Results

3.1 | Bird Flight Speeds

The literature review allowed the compilation of flight speeds for 140 species, estimated with radar (135 species), ornithodolite (32 species), satellite, and GPS telemetry (5 species) (some species had been recorded with several methods). This data was mostly recorded during migration (88% of studies). Using the Movebank database, we collected groundspeed data for 31 additional species. For 17 species (belonging to 15 families and 5 orders) for which there was no published data or GPS tracking, we computed the theoretical airspeed using the Flight program.

In total, we built a database for 168 species (ESM 04). The groundspeed in local flights ranged from $6.3 \, \mathrm{m\,s^{-1}} \pm 0.2$ SD for Montagu's harrier (*C. pygargus*) in local (hunting) flights to 21.4 ± 2.4 SD $\mathrm{m\,s^{-1}}$ for the mallard (*Anas platyrhynchos*). The groundspeed in migratory flights ranged from $6.7 \, \mathrm{m\,s^{-1}} \pm 1.0$ SD for both the Eurasian siskin (*Carduelis spinus*) and Eurasian jay (*Garrulus glandarius*) to 22.1 ± 4 SD $\mathrm{m\,s^{-1}}$ for the common scoter (*Melanitta nigra*).

3.2 | Turbine Shutdown Time $T_{shutdown}$

Overall, 137 experimental shutdowns were performed at seven WEF. The analysis of correlations between the five potential explanatory variables (ESM 03) resulted in the selection of three variables for modelling rotor shutdown probability and $T_{shutdown}$: blade length, initial wind speed, and machine type (synchronous vs. asynchronous). The other variables (nacelle height and initial turbine rotation speed) were too correlated (see ESM 03) with these three variables to be tested simultaneously in the models.

The probability that the residual rotation speed was ≤ 2 rpm was related to blade length and initial wind speed (ESM 03). For the turbines that reached the 3 or 2 rpm values before 90 s, once the shutdown command was initiated at the SCADA, it took an average of $32.2 \, \mathrm{s} \pm 13.5$ SD [range 15–55 s] and $38.8 \, \mathrm{s} \pm 14.5$ SD [range 15–65 s] for the residual rotation speed to reach 3 and 2 rpm, respectively. Modelling of the $T_{shutdown}$ for the 3- and 2-rpm thresholds showed that machine type, blade length, initial wind speed, and the interaction of the latter two variables significantly affected the time required to reach these residual rotation speeds. These variables explained 57% and 49% of the variance in the dataset for the 3- and 2-rpm thresholds, respectively.

The time for the rotor to decelerate and reach the 3- and 2-rpm thresholds was longer when blade length was longer (Figure 2A),
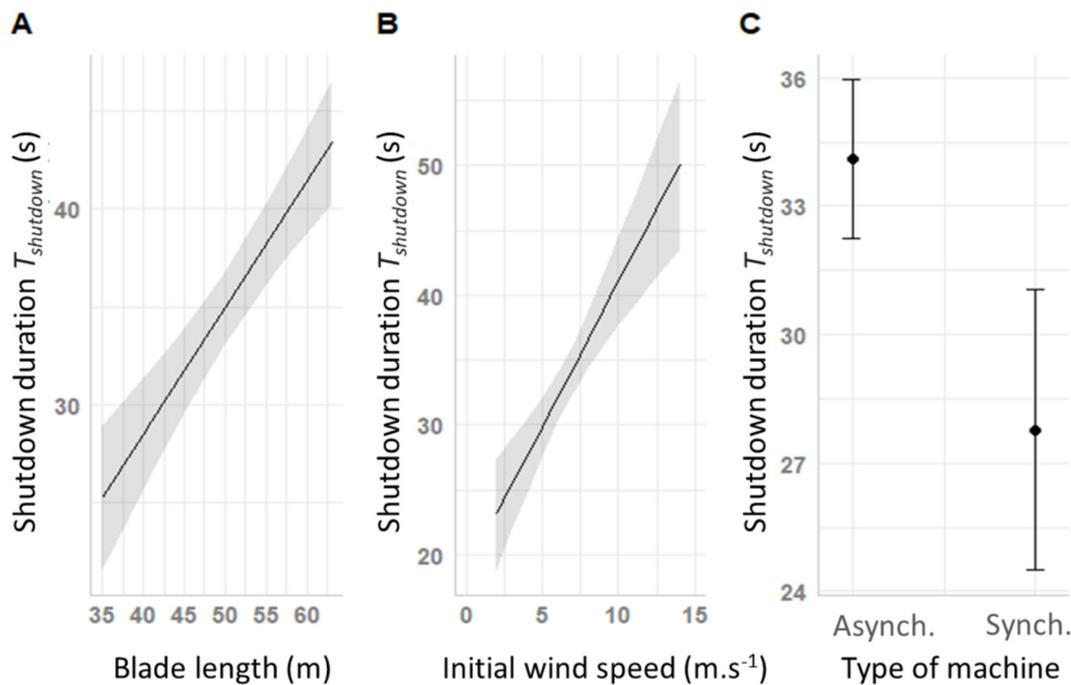
FIGURE 2 | Turbine shutdown time $T_{shutdown}$ required for the residual rotation speed to reach ≤ 3 rpm in 90 s as a function of (A) blade length, (B) initial wind speed, and (C) turbine type (Asynch = asynchronous, Synch. = synchronous). The shaded areas represent the 95% confidence intervals of the estimates. Because the model included an interaction, each variable that is not represented was set to its mean, and the machine type was asynchronous. The pattern was similar at a residual rotation speed of 2 rpm.

when wind speed was higher (Figure 2B), and if the machine was asynchronous (Figure 2C). The significant interaction between turbine blade length and initial wind speed implied that for a given initial wind speed, the rotor decelerated differently depending on the blade length. In the presence of a 5 m s^{-1} wind, $T_{shutdown}$ was identical, whatever the blade length. But in the presence of wind between 10 and 20 m s^{-1}, the longer the blade length, the longer the time needed for the rotor to reach the residual rotation speed.

3.3 | Examples of Cautionary Detection Distances

3.3.1 | Effect of Type of Flight, Turbine Characteristics, Wind Speed, and Residual Rotation Speed

For the first case study with the lesser kestrel, $T_{shutdown}$ of asynchronous turbines with a 35-m blade length varied between 18 and 23 s according to the residual rotation speed threshold chosen (2 or 3 rpm) (Table 1). Similarly, for asynchronous turbines with a 41-m blade length, $T_{shutdown}$ was increased by 10 s. In a local flight context, D varied between 315–360 m for the 35-m blades and 435–490 m for the 41-m blades (Table 1). In a migratory context, lesser kestrels fly on average at a speed 146% faster than in local flight, resulting in an increase in D of 135% for the 35-m blades and 137% for the 41-m blades (Table 1). A screen view of one calculation from the *Eoldist* application is shown in Figure 1.

We tested the effect of wind speed, type of machine, and blade length on D for lesser kestrels in local flight. At a wind speed of 5 m s^{-1}, $T_{shutdown}$ varied mostly according to the type

of machine (longer with asynchronous machines than synchronous), but not with blade length (slope close to zero). Therefore, D was not strongly affected by blade length but was ~130% larger for asynchronous machines (Figure 3). The effect of blade length was more pronounced at wind speeds of 10 m s^{-1} (larger slope coefficients) (Figure 3). The difference in machine type was minor (< 5%) at 10 m s^{-1} and was reversed at 15 m s^{-1} (asynchronous machines shut down faster at 15 m s^{-1}, hence resulting in a 10% decrease in D).

3.3.2 | Effect of Percentage of Detected Flights

When choosing a median threshold of flights detected (50%), estimates of D were similar at 610–615 m for both Bewick's swan and the griffon vulture (Figure 4). For the swan, whose variance in groundspeed is low, the range of D varied between 565 and 725 m for, respectively, 25% and 95% of flights detected. For the vulture, whose variance in groundspeed is high, the range of D varied between 450 and 1020 m for, respectively, 25% and 95% of flights detected.

3.3.3 | Effect of Shutdown Time

The first set of calculations was for an asynchronous machine with a blade length of 45 m and an initial wind speed of 10 m s^{-1}. With a residual rotation speed of 3 rpm (corresponding to a linear speed at the blade tip of 51 km h^{-1}), $T_{shutdown}$ would take 33.8 s $\pm$ 2.4. With a threshold of 95% of flights detected, D for these species would range from 370 m for Montagu's harrier to 1020 m for the griffon vulture (Figure 5).

For larger wind turbines (asynchronous machine, 63-m blade), applying a conservative precautionary principle with a residual rotation speed of 2 rpm (to stay within the limit of a linear blade tip speed corresponding to 50 km h^{-1}), calculations give a $T_{shutdown}$ of 69.9 s ± 3.3. With a detection threshold of 95%, D almost doubled for all species. Thus, to protect almost all flights of Montagu's harriers, they would have to be detected at 650 m, and griffon vultures at 1915 m (Figure 5).

4 | Discussion

Eoldist is an interactive dashboard (developed using the Shiny package in R) that calculates the cautionary detection distance D required to effectively shut down wind turbines to reduce collision risks for a selected species. It is freely available online, both in English (https://shiny.cefe.cnrs.fr/en_Eoldist/) and in French (https://shiny.cefe.cnrs.fr/Eoldist/). It includes a database of bird flight speeds and a statistical model to predict turbine shutdown time.

4.1 | Bird Flight Speed

The user can choose from 168 bird species included in the application for which flight speeds have either been documented or estimated with aerodynamic and morphological models. This bird flight speed database is currently limited to Western Palearctic species, as the application was developed in the framework of the French Reduction of Avian Mortality

TABLE 1 | Effect of flight context and blade length for detection distance of a lesser kestrel.

Flight context	Flight speed (mean ± SD; in m s^{-1})	Blade length (m)	$T_{shutdown}$ (mean ± SD; in s) to reach 3 rpm	$T_{shutdown}$ (mean ± SD; in s) to reach 2 rpm	D (m) at 3 rpm	D (m) at 2 rpm
Local	7.7 ± 1.8	35	18.9 ± 3.7	23.2 ± 4.4	315	360
		41	28.7 ± 2.7	33.2 ± 3.2	435	480
Migratory	11.3 ± 2.8	35	18.9 ± 3.7	23.2 ± 4.4	425	490
		41	28.7 ± 2.7	33.2 ± 3.2	595	670

Note: Estimates of cautionary detection distances D for the lesser kestrel (*Falco naumanni*) at a wind energy facility including two types of asynchronous turbines, in a context of local flight or migratory flight. Two residual rotation speeds (3 and 2 rpm) were tested and resulted in different shutdown times $T_{shutdown}$ and cautionary detection distances. All simulations were computed with an initial wind speed of 10 m s^{-1} and a flight detection of 95%.
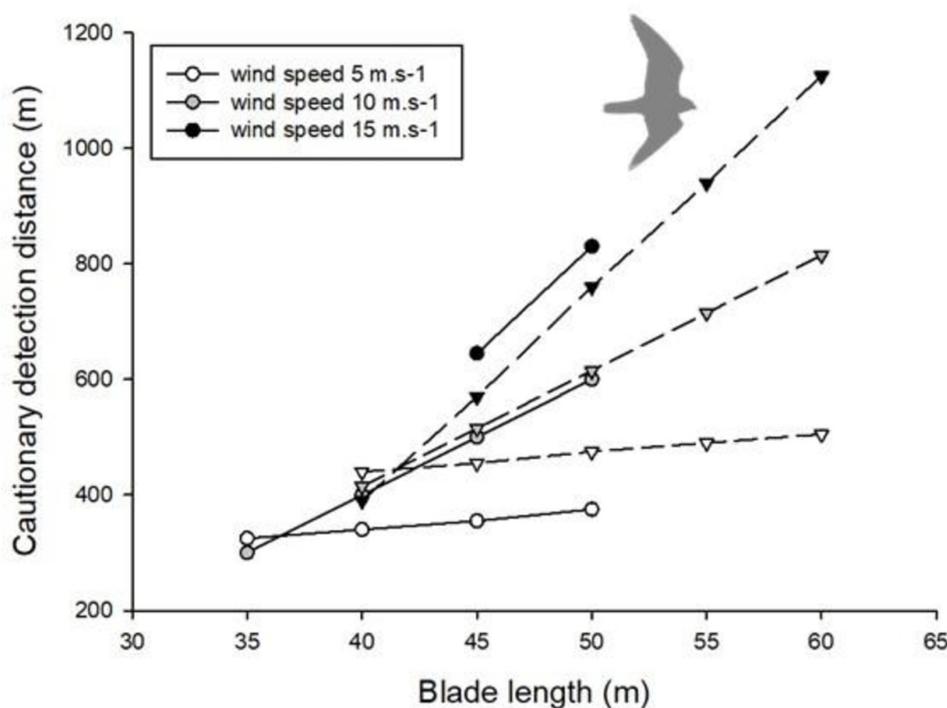

FIGURE 3 | Effect of blade length, type of machine (synchronous: circles; asynchronous: triangles), and wind speed (5, 10, and 15 m s^{-1}) on cautionary detection distance D of the lesser kestrel (*Falco naumanni*) in local flight. The effect of wind speed is due to changes in $T_{shutdown}$ (and not in-flight speed). Simulations were performed with 95% of detected flights and a residual rotation speed of 3 rpm.

in Operating Wind Energy Facilities (MAPE) research program (https://mape.cnrs.fr/) funded by French agencies and WEF companies operating in France. In coming years, it is likely that more flight speeds will be published on birds made possible by the miniaturization of GPS tags, allowing them to be deployed on smaller species. In addition, the database can be updated by integrating flight speeds measured for birds from other continents.
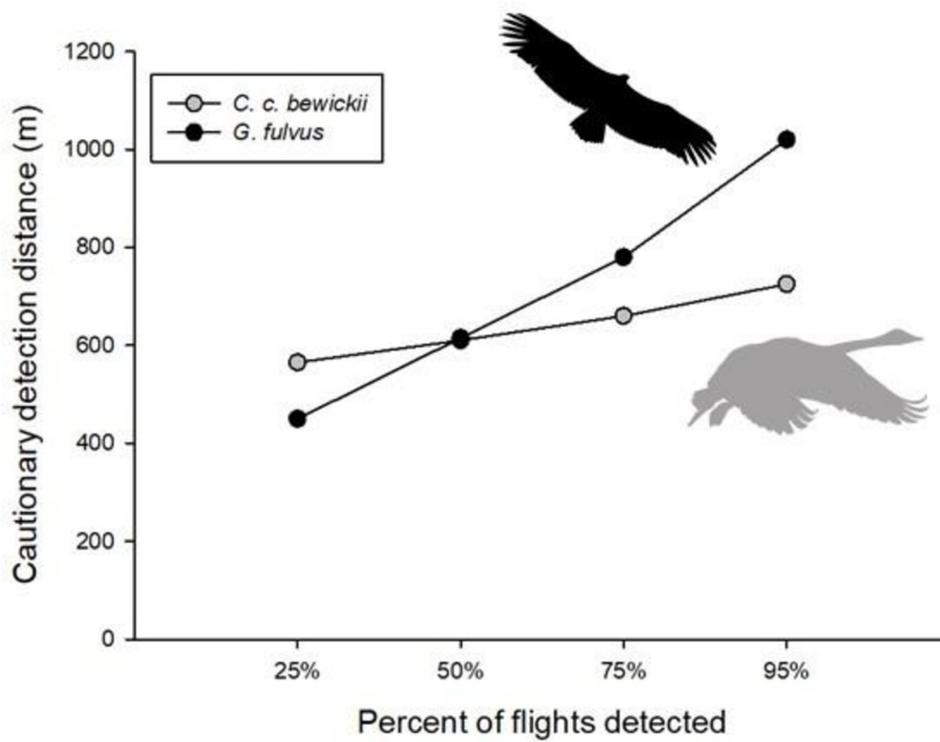

FIGURE 4 | Effect of the percentage of detected flights on cautionary detection distances for two species differing in flight speed variance: Bewick's swan (*Cygnus columbianus bewickii*) (groundspeed $15.2 \pm 0.7\,\mathrm{m\,s^{-1}}$) and the griffon vulture (*Gyps fulvus*) (groundspeed $15.3 \pm 5.3\,\mathrm{m\,s^{-1}}$). Simulations were performed with asynchronous turbines with 45-m blades, an initial wind speed of $10\,\mathrm{m\,s^{-1}}$, and a residual rotation speed of 3 rpm, resulting in a turbine shutdown time of $35.2 \pm 2.1\,\mathrm{s}$.
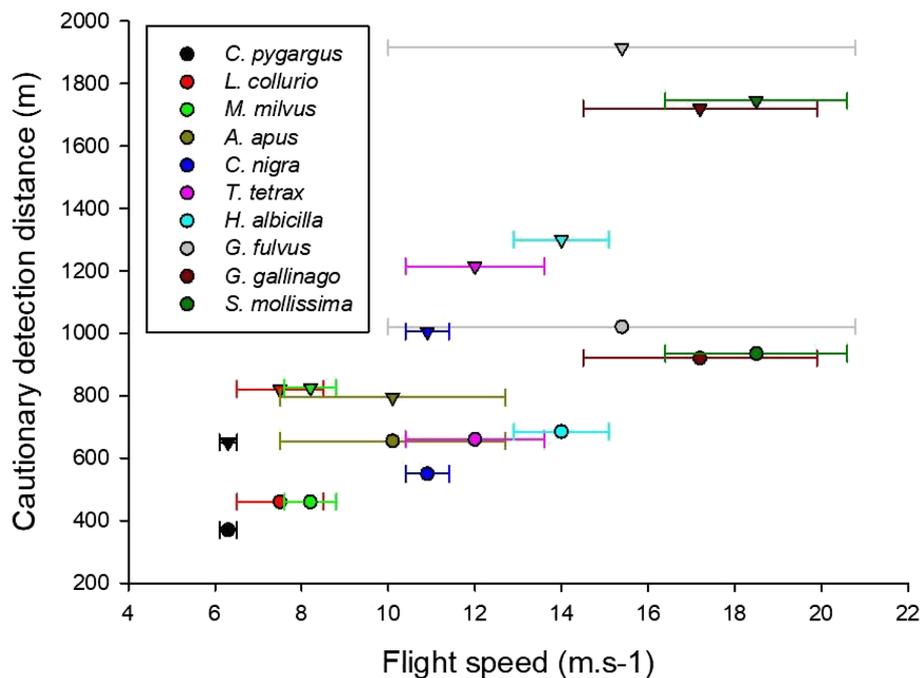

FIGURE 5 | Cautionary detection distance D as a function of blade length for 10 species of conservation concern in Europe. Variations in mean flight speed affect D with asynchronous turbines with 45-m blades (circles) and 63-m blades (triangles). All simulations were performed with an initial wind speed of $10\,\mathrm{m\,s^{-1}}$, a residual rotation speed of 3 rpm and 95% of flights detected.

Two key features of the database and the web application are the integration of the frequency distribution of flight speeds and the flight context. In reviewing the numerous intrinsic and external factors that can affect flight speed (ESM 01), we assumed that variation in flight speed for a given species is almost as important as its average speed. Theoretical knowledge on the mechanics of avian flight demonstrates that birds can choose between a limited range of airspeeds to stay airborne [22]. In the context of collisions with static anthropic infrastructure, the important referential is not the air mass in which the bird moves, but the ground where the infrastructure is installed; the movements of the air mass can contribute to increasing or decreasing flight speed relative to the ground and the infrastructure concerned [25]. Thus, it is crucial that a bird's groundspeed and natural variations in speed are taken into account rather than only airspeed, as is common in large-scale studies of bird flight aerodynamics (e.g., [29, 30]).

Our choice of using groundspeed rather than airspeed allows us to incorporate all situations when birds fly headwind, crosswind, tailwind, and in still air. It has been shown that birds generally prefer using tailwind during migration [39–41], hence groundspeeds may be increased, and that is what we generally observed when comparing values for migratory versus local flight in *Eoldist*. Yet in some situations migratory birds may cross air layers with headwind close to the ground (particularly in mountain areas) before reaching better wind conditions at higher altitudes (e.g., [42–44]. Migration can start in tailwinds but end up in headwinds; see, for example, [45]. Furthermore, when large birds take off, they always fly headwind to improve lift and increase airspeed and then eventually change direction to fly tailwind (e.g., in shags *Phalacrocorax aristotelis*, [46]). So, in the first hundred meters above ground (below or within the rotor swept height), wind support can be different than at higher heights. Using only airspeed and full tailwind as the main hypothesis to estimate *D* would thus be quite restrictive and potentially leading to decision errors regarding the distance needed to shutdown wind turbines to prevent (most) collisions. Using groundspeed, our estimate of *D* incorporates all environmental factors that modulate this speed. We nevertheless implicitly assume that windspeed distribution at the turbine location is similar to the windspeed distribution at the location where birds have been recorded.

Flight context can also result in differences in a bird's flight speed. Previous studies have shown differences in flight speed between local flights and migratory flights (e.g., [27, 47]) and also between pre- and post-nuptial migrations [30, 48]. Whereas birds that use flapping flight have a limited range of flight speeds, species that use soaring/gliding flight can typically alternate between slow speeds when soaring and fast speeds when gliding [35, 49]. Consequently, the variance in flight speed is typically larger in soaring/gliding species than in flapping species. This in turn has implications for *D* when varying the percentage of flights detected: for species with larger groundspeed variance, *D* greatly increased because of the extended "upper-tail" of the distribution when applying the precautionary principle of 95% of flights detected (as in our example of Bewick's swan and the griffon vulture: Figure 5).

4.2 | Shutdown Time Experiments

To our knowledge, wind turbine deceleration time triggered by an ADS has not been investigated in the literature. We found only a few engineering papers describing emergency shutdowns and their effects on the blades and generator [50, 51]; these studies indicate that emergency shutdowns take between 5 and 15 s and can severely alter wind turbine structure. This explains why engineers are reluctant to apply rapid emergency shutdowns regularly to prevent bird collisions, preferring smoother and slower shutdowns by spinning the blades against the wind.

This lack of data meant that we had to perform our own field experiments with the help of volunteer WEF operators. These experiments concerned mainly asynchronous machines. It should be noted that the asynchronous machines tested had longer blade lengths than the synchronous turbines tested, resulting in a confounding factor in the analysis. In addition, very few tests were performed in wind conditions $> 10\,\text{m\,s}^{-1}$, and of these, most were performed on synchronous machines. The results of the following analyses should thus be interpreted with caution due to these imbalances in experimental conditions. Improving this estimate of $T_{shutdown}$ is our priority, and we will thus update *Eoldist* as soon as we get improved estimates. Hopefully this publication may facilitate future collaboration, providing an opportunity to repeat the experiment in additional WEF and more turbine types and more wind conditions.

The turbine shutdown time tests conducted showed that, overall, synchronous wind turbines can be shut down 5–10 s faster than asynchronous wind turbines. The average $T_{shutdown}$ to reach the threshold values of 3 and 2 rpm were 32 and 39 s, respectively. However, these values depended on the blade length, the initial wind speed, and especially on the interaction between these two variables. Our analyses showed, for example, that winds of $10\,\text{m\,s}^{-1}$ and large blades could increase $T_{shutdown}$ to values of 50 s and even to almost 100 s for wind speeds of $15\,\text{m\,s}^{-1}$. The issue of extended shutdown times is further deepened by the fact that birds may travel faster in these windy conditions (if tailwind), thus highlighting a limitation in the effectiveness of ADS. The pitch rate, that is, the speed at which blades are spun against the wind to decelerate the rotor, was certainly an important but missing factor to model $T_{shutdown}$, and the lack of this value in the models could potentially explain the relatively large residual variance we obtained. Improving pitch rate to make blades spin more quickly may be a promising way to reduce $T_{shutdown}$ and improve the mitigation of bird collisions.

If a user lacks knowledge about $T_{shutdown}$, *Eoldist* offers a solution for estimating turbine shutdown time solely on the basis of wind and turbine characteristics. If a user has more precise knowledge of $T_{shutdown}$ at a particular WEF, it is also possible to manually enter a value for $T_{shutdown}$. This feature makes *Eoldist* flexible and adaptable to the wide range of situations currently encountered in WEF.

4.3 | Concluding Remarks

The *Eoldist* application allows a user to modify two important parameters (see below) in determining what distance a species

11 of 15

of bird needs to be detected in order to avoid collision by triggering a turbine shutdown. These two parameters can have a very significant effect on the output, and they depend as much on policy and societal choices as on bird biology.

The first parameter is the wind turbine's residual speed after a shutdown order, which is never equal to 0 rpm in case of a shutdown to avoid bird collision, in contrast to an emergency shutdown. Wind turbine manufacturers generally consider a turbine to be "shut down" when it rotates at a residual speed of < 2 or 3 rpm [52]. However, the longer the blades, the greater the linear speed at the tip of the blade; for a 60-m-long blade, the blade tip's linear speed is equal to 50 km h^{-1} at a rotation speed of 2 rpm. The risk of collision thus cannot be completely eliminated even when wind turbines are considered "stationary" according to the criteria currently in force. Our example with the lesser kestrel (Table 1) illustrates how applying a more restrictive threshold (2 rpm instead of 3 rpm) increases $T_{shutdown}$ and consequently increases the D required.

The second parameter is flight detection, which the user can select at a threshold between 5% and 95%. If a threshold of 50% is chosen, *Eoldist* will estimate a D that should detect a bird and have enough time to shut down the turbine in 50% of cases, based on the frequency distribution of bird groundspeeds. But is such a threshold ethically tolerable for rare and protected species because it implies that in 50% of cases, these birds will risk collision? Environmental laws protecting species in many western countries prohibit a single mortality. This would make it necessary to use a higher threshold (e.g., 95%) to calculate a more conservative D for a protected species to comply with the legislation in force. Our general advice would be to increase the threshold for rare and highly protected species (in which every casualty may lead to local population extinction) and decrease it for more common species, with a lower protection level, in which a few casualties would not threaten the local population. Our case studies with swans and vultures illustrate how much D can increase when applying the precautionary principle of a threshold of 95% of detected flights. This effect was more pronounced for species with large variance in flight speed, which is typical of large soaring/gliding birds such as raptors and storks.

Finally, our field experiments revealed that $T_{shutdown}$ was highly correlated to blade length and initial wind speed. With the current trend of increased blade length to achieve higher performance and energy output when repowering old WEF or planning new WEF [53], we can hypothesize that $T_{shutdown}$ will also increase if future wind turbines are built using the same principles and materials. *Eoldist* allows the prediction of the effect of such a blade length increase on D. In the case of the lesser kestrel (Figure 3), we found that doubling the blade length resulted in a two- to threefold increase in D, depending on initial wind speed. When comparing a set of 10 bird species of various sizes (Figure 5), the same pattern holds true. By increasing blade length from 45 to 63 m, $T_{shutdown}$ doubled, and consequently D increased by several hundred meters. For example, to protect almost all Montagu's harriers (small) and griffon vultures (large), they would have to be detected at 650 and 1915 m, respectively, with the 63-m blades, and at 370 and 1020 m, respectively, for 45-m blades. This raises the question of the technical feasibility of detecting birds at such distances. Current ADS technologies, which mainly rely on optical cameras, can certainly detect these species at the distances estimated for 45-m blades, but probably not at that estimated for the 63-m blades. In the only optic-based ADS scientifically assessed to date, the mean detection distance of large eagles was 793 m (2.5 and 97.5 percentiles = 269–1191 m); other birds were detected at 383 m on average [12]. For the golden eagle (*Aquila chrysaetos*) in local flight for turbines corresponding to those described by McClure, Martinson, and Allison [12] (L_{blade} = 50 m, assuming asynchronous machines and wind speed of 10 m s^{-1}), *Eoldist* estimated a D of 945 m at a detection threshold of 95%, which is compatible with the detection values reported above. Increasing detection distances can be achieved by using long focal lenses, which are however difficult to combine with the wide-angle coverage needed to detect birds from any direction and height. At the moment, only an ADS using radar is likely to be able to detect smaller birds at distances of more than 1000 m together with a wide-angle coverage [13]. For migratory corridors, where bird flight trajectories are predictable, another option to increase D would require installing ADS not in the WEF but a few hundred meters ahead of the WEF.

While detecting birds at further distances should help reduce collision risk, this would be at the expense of energy production. In *Eoldist*, as a precautionary principle, we assumed that the target bird follows a straight-line trajectory towards the wind turbine with no reaction in this trajectory (e.g., no behavioral response to a noise deterrent). However, increasing detection distance and triggering shutdown earlier may increase the likelihood that birds change direction for any reason while the turbine is decelerating, hence making the shutdown useless and therefore costly. Improving bird collision mitigation while maintaining high energy production without frequent turbine shutdowns will require better classification algorithms that quickly and reliably identify risky trajectories that justify shutdown and those where shutdown is not required.

The trajectory of birds in relation to the rotor plane may also affect their approaching groundspeed and the way to estimate D. Assuming that the rotor plane is always perpendicular to the wind direction (necessary for maximal energy production), if collisions always occur with tailwind while birds fly in the same direction as the wind, it would be best to use the sum of airspeed and wind speed and remove blade length from Equation (1). If collisions always occur when birds fly crosswind, that is, perpendicular to wind direction and parallel to the rotor plane, then Equation (1) should remain as it is, including blade length, and using either groundspeed or airspeed would yield similar results for estimating D. The reality probably lies in-between, and it is likely that there is a mix of bird trajectories (between these two extreme cases) that can lead to collisions with turbines. However, to our knowledge, there is no published study on bird trajectories before collisions, relative to wind direction and rotor plane. Also, avoidance behavior may change according to trajectory and wind support, as shown in Black kites (*Milvus migrans*) that display higher avoidance behavior for wind perpendicular to the rotor [54]. With such a gap of knowledge, using a precautionary principle, we thus preferred using overall groundspeed, including blade length in Equation (1), to account for every possible trajectory and wind direction.

In conclusion, the calculations performed with *Eoldist* show how much work remains to be done by the agencies in charge of protecting biodiversity and by the wind turbine industry as a whole to define turbine shutdown speeds and flight detection thresholds that are compatible with the regulatory protection of birds while remaining within limits that are technically achievable by ADS suppliers. The planned increase in size of wind turbines (both onshore and offshore) is likely to greatly increase the risk of collision if technical solutions are not found to (1) increase the detection distance of ADSs or improve the algorithms to better predict trajectories at risk, and/or (2) improve braking to greatly reduce turbine shutdown time. Because increasing detection distances with wide-angle coverage is problematic, it would probably be more efficient to improve turbine deceleration time in order to reduce cautionary detection distance. In the meantime, *Eoldist* can help stakeholders determine where local conditions of WEF and/or focal species warrant the installation of an ADS to reduce collisions and where local conditions make detection at a reasonable distance problematic or unlikely to be achieved, making the deployment of an ADS inefficient in reducing collision risks.

Data Availability Statement

The source code and the bird flight speed databases are freely accessible at the CNRS Gitlab URL https://src.koda.cnrs.fr/cefe/hair/eoldist/-/tree/main/eoldist_EN?ref_type=heads.

References

1. S. Teske, *Achieving the Paris Climate Agreement Goals: Global and Regional 100% Renewable Energy Scenarios With Non-Energy GHG Pathways for +1.5°C and + 2°C* (Cham, Switzerland: Springer Nature, 2019).

2. M. R. Perrow, *Wildlife and Wind Farms, Conflicts and Solutions: Vol. 1: Onshore: Potential Effects* (Exeter, UK: Pelagic Publishing, 2017).

3. A. T. Marques, H. Batalha, and J. Bernardino, "Bird Displacement by Wind Turbines: Assessing Current Knowledge and Recommendations for Future Studies," *Birds* 2, no. 4 (2021): 460–475, https://doi.org/10.3390/birds2040034.

4. A. T. Marques, C. D. Santos, F. Hanssen, et al., "Wind Turbines Cause Functional Habitat Loss for Migratory Soaring Birds," *Journal of Animal Ecology* 89, no. 1 (2020): 93–103, https://doi.org/10.1111/1365-2656.12961.

5. M. De Lucas, G. F. E. Janss, and M. Ferrer, *Birds and Wind Farms; Risk Assessment and Mitigation* (Madrid, Spain: Quercus, 2007).

6. J. Köppel, *Wind Energy and Wildlife Interactions* (Berlin Heidelberg: Springer, 2017).

7. C. B. Thaxter, G. M. Buchanan, J. Carr, et al., "Bird and Bat Species' Global Vulnerability to Collision Mortality at Wind Farms Revealed Through a Trait-Based Assessment," *Proceedings of the Royal Society B: Biological Sciences* 284, no. 1862 (2017): 20170829, https://doi.org/10.1098/rspb.2017.0829.

8. O. Duriez, P. Pilard, N. Saulnier, P. Boudarel, and A. Besnard, "Windfarm Collisions in Medium-Sized Raptors: Even Increasing Populations Can Suffer Strong Demographic Impacts," *Animal Conservation* 26, no. 2 (2023): 264–275, https://doi.org/10.1111/acv.12818.

9. T. J. Conkling, H. B. Vander Zanden, T. D. Allison, et al., "Vulnerability of Avian Populations to Renewable Energy Production," *Royal Society Open Science* 9, no. 3 (2022): 211558, https://doi.org/10.1098/rsos.211558.

10. T. E. Katzner, D. M. Nelson, J. E. Diffendorfer, et al., "Wind Energy: An Ecological Challenge," *Science (New York, N.Y.)* 366, no. 6470 (2019): 1206–1207.

11. D. Serrano, A. Margalida, J. M. Pérez-García, et al., "Renewables in Spain Threaten Biodiversity," *Science* 370, no. 6522 (2020): 1282–1283, https://doi.org/10.1126/science.abf6509.

12. C. J. W. McClure, L. Martinson, and T. D. Allison, "Automated Monitoring for Birds in Flight: Proof of Concept With Eagles at a Wind Power Facility," *Biological Conservation* 224 (2018): 26–33, https://doi.org/10.1016/j.biocon.2018.04.041.

13. R. Tomé, F. Canario, A. H. Leitão, and N. Pires, "Radar Assisted Shutdown on Demand Ensures Zero Soaring Bird Mortality at a Wind

Farm Located in a Migratory Flyway," in *Wind Energy and Wildlife Interactions*, ed. J. Köppel (Berlin Heidelberg: Springer, 2017), 119–134.

14. A. E. Duerr, A. E. Parsons, L. R. Nagy, M. J. Kuehn, and P. H. Bloom, "Effectiveness of an Artificial Intelligence-Based System to Curtail Wind Turbines to Reduce Eagle Collisions," *PLoS ONE* 18, no. 1 (2023): e0278754, https://doi.org/10.1371/journal.pone.0278754.

15. J. Niemi and J. T. Tanttu, "Deep Learning–Based Automatic Bird Identification System for Offshore Wind Farms," *Wind Energy* 23, no. 6 (2020): 1394–1407, https://doi.org/10.1002/we.2492.

16. C. J. W. McClure, B. W. Rolek, L. Dunn, J. D. McCabe, L. Martinson, and T. Katzner, "Eagle Fatalities Are Reduced by Automated Curtailment of Wind Turbines," *Journal of Applied Ecology* 58, no. 3 (2021): 446–452, https://doi.org/10.1111/1365-2664.13831.

17. C. J. W. McClure, B. W. Rolek, L. Dunn, J. D. McCabe, L. Martinson, and T. E. Katzner, "Confirmation That Eagle Fatalities Can Be Reduced by Automated Curtailment of Wind Turbines," *Ecological Solutions and Evidence* 3, no. 3 (2022): e12173, https://doi.org/10.1002/2688-8319.12173.

18. M. Huso and D. Dalthorp, "Reanalysis Indicates Little Evidence of Reduction in Eagle Mortality Rate by Automated Curtailment of Wind Turbines," *Journal of Applied Ecology* 60, no. 10 (2023): 2282–2288, https://doi.org/10.1111/1365-2664.14196.

19. T. Raynal-Ehrke, *Anforderungen an Eine Fachlich Valide Erprobung von Technischen Systemen zur Bedarfsgerechten Betriebsregulierung von Windenergieanlagen*, (KNE-19-04; p. 31) (Kompetenzzentrum Naturschutz und Energiewende, 2019).

20. T. Alerstam, M. Rosén, J. Bäckman, P. G. P. Ericson, and O. Hellgren, "Flight Speeds Among Bird Species: Allometric and Phylogenetic Effects," *PLoS Biology* 5, no. 8 (2007): e197.

21. U. M. Norberg, "How a Long Tail and Changes in Mass and Wing Shape Affect the Cost for Flight in Animals," *Functional Ecology* 9 (1995): 48–54.

22. C. J. Pennycuick, *Modelling the Flying Bird* (London, UK: Academic Press, 2008).

23. J. J. Videler, *Avian Flight* (Oxford, UK: Oxford University Press, 2005).

24. F. Liechti, "Birds: Blowin' by the Wind?," *Journal of Ornithology* 147, no. 2 (2006): 202–211.

25. K. Safi, B. Kranstauber, R. Weinzierl, et al., "Flying With the Wind: Scale Dependency of Speed and Direction Measurements in Modelling Wind Support in Avian Flight," *Movement Ecology* 1, no. 1 (2013): 4.

26. L. B. Spear and D. G. Ainley, "Flight Behaviour of Seabirds in Relation to Wind Direction and Wing Morphology," *Ibis* 139, no. 2 (1997): 221–233.

27. R. Harel, O. Duriez, O. Spiegel, et al., "Decision-Making by a Soaring Bird: Time, Energy and Risk Considerations at Different Spatio-Temporal Scales," *Philosophical Transactions of the Royal Society of London B: Biological Sciences* 371, no. 1704 (2016): 20150397, https://doi.org/10.1098/rstb.2015.0397.

28. B. Bruderer, "Three Decades of Tracking Radar Studies on Bird Migration in Europe and the Middle East," in *Migrating Birds Know No Boundaries*, eds. Y. Leshem, Y. Mandelik, and J. Shamoun-Baranes (Latrun, Israel: International Center for the Study of Bird Migration, 1999), 107–141.

29. B. Bruderer and A. Boldt, "Flight Characteristics of Birds: I. Radar Measurements of Speeds," *Ibis* 143, no. 2 (2001): 178–204, https://doi.org/10.1111/j.1474-919X.2001.tb04475.x.

30. C. Nilsson, R. H. G. Klaassen, and T. Alerstam, "Differences in Speed and Duration of Bird Migration Between Spring and Autumn," *American Naturalist* 181, no. 6 (2013): 837–845, https://doi.org/10.1086/670335.

31. C. J. Pennycuick, "The Flight of Petrels and Albatrosses (Procellariformes), observed in South Georgia and Its Vicinity," *Philosophical Transactions of the Royal Society of London, Series B* 300 (1982): 75–106.

32. A. Hedenström and S. Åkesson, "Adaptive Airspeed Adjustment and Compensation for Wind Drift in the Common Swift: Differences Between Day and Night," *Animal Behaviour* 127 (2017): 117–123.

33. C. J. Pennycuick, S. Akesson, and A. Hedenström, "Air Speeds of Migrating Birds Observed by Ornithodolite and Compared With Predictions From Flight Theory," *Journal of the Royal Society Interface* 10 (2013): 20130419, https://doi.org/10.1098/rsif.2013.0419.

34. E. S. Bridge, K. Thorup, M. S. Bowlin, et al., "Technology on the Move: Recent and Forthcoming Innovations for Tracking Migratory Birds," *Bioscience* 61, no. 9 (2011): 689–698, https://doi.org/10.1525/bio.2011.61.9.7.

35. N. Horvitz, N. Sapir, F. Liechti, R. Avissar, I. Mahrer, and R. Nathan, "The Gliding Speed of Migrating Birds: Slow and Safe or Fast and Risky?," *Ecology Letters* 17, no. 6 (2014): 670–679, https://doi.org/10.1111/ele.12268.

36. C. Pennycuick, "Speeds and Wingbeat Frequencies of Migrating Birds Compared With Calculated Benchmarks," *Journal of Experimental Biology* 204, no. 19 (2001): 3283–3294.

37. A. Tanferna, L. Lopez-Jimenez, J. Blas, F. Hiraldo, and F. Sergio, "Different Location Sampling Frequencies by Satellite Tags Yield Different Estimates of Migration Performance: Pooling Data Requires a Common Protocol," *PLoS ONE* 7, no. 11 (2012): e49659.

38. Birdlife International, *European Red List of Birds 2021* (Luxembourg: Publication Office of the European Union, 2022), https://doi.org/10.2779/959320.

39. P. Becciu, D. Troupin, L. Dinevich, Y. Leshem, and N. Sapir, "Soaring Migrants Flexibly Respond to Sea-Breeze in a Migratory Bottleneck: Using First Derivatives to Identify Behavioural Adjustments Over Time," *Movement Ecology* 11, no. 1 (2023): 44, https://doi.org/10.1186/s40462-023-00402-4.

40. M. Mateos-Rodriguez and F. Liechti, "How Do Diurnal Long-Distance Migrants Select Flight Altitude in Relation to Wind?," *Behavioral Ecology* 23, no. 2 (2012): 403–409, https://doi.org/10.1093/beheco/arr204.

41. U. Mellone, R. H. G. Klaassen, C. Garcia-Ripolles, et al., "Interspecific Comparison of the Performance of Soaring Migrants in Relation to Morphology, Meteorological Conditions and Migration Strategies," *PLoS ONE* 7, no. 7 (2012): e39833.

42. L. A. Hawkes, S. Balachandran, N. Batbayar, et al., "The Trans-Himalayan Flights of Bar-Headed Geese (*Anser indicus*)," *Proceedings of the National Academy of Sciences* 108, no. 23 (2011): 9516–9519, https://doi.org/10.1073/pnas.1017295108.

43. K. Thorup, T. Alerstam, M. Hake, and N. Kjellen, "Traveling or Stopping of Migrating Birds in Relation to Wind: An Illustration for the Osprey," *Behavioral Ecology* 17, no. 3 (2006): 497–502, https://doi.org/10.1093/beheco/arj054.

44. R. Villegas-Patraca and L. Herrera-Alsina, "Migration of Franklin's Gull (*Leucophaeus pipixcan*) and Its Variable Annual Risk From Wind Power Facilities Across the Tehuantepec Isthmus," *Journal for Nature Conservation* 25 (2015): 72–76, https://doi.org/10.1016/j.jnc.2015.03.006.

45. J. Geisler, J. Madsen, B. A. Nolet, and K. H. Schreven, "Sea Crossings of Migratory Pink-Footed Geese: Seasonal Effects of Winds on Flying and Stopping Behaviour," *Journal of Avian Biology* 2022, no. 10 (2022): e02985.

46. Y. Kogure, K. Sato, Y. Watanuki, S. Wanless, and F. Daunt, "European Shags Optimize Their Flight Behavior According to Wind Conditions," *Journal of Experimental Biology* 219, no. 3 (2016): 311–318, https://doi.org/10.1242/jeb.131441.

47. D. Pinaud, "Quantifying Search Effort of Moving Animals at Several Spatial Scales Using First-Passage Time Analysis: Effect of the Structure

of Environment and Tracking Systems," *Journal of Applied Ecology* 45, no. 1 (2008): 91–99, https://doi.org/10.1111/j.1365-2664.2007.01370.x.

48. T. Alerstam, "Bird Flight and Optimal Migration," *Trends in Ecology & Evolution* 6, no. 7 (1991): 210–215.

49. H. J. Williams, A. J. King, O. Duriez, L. Börger, and E. L. C. Shepard, "Social Eavesdropping Allows for a More Risky Gliding Strategy by Thermal-Soaring Birds," *Journal of the Royal Society Interface* 15, no. 148 (2018): 20180578, https://doi.org/10.1098/rsif.2018.0578.

50. E. E. Bachynski, M. Etemaddar, M. I. Kvittem, C. Luan, and T. Moan, "Dynamic Analysis of Floating Wind Turbines During Pitch Actuator Fault, Grid Loss, and Shutdown," *Energy Procedia* 35 (2013): 210–222.

51. Z. Jiang, M. Karimirad, and T. Moan, "Dynamic Response Analysis of Wind Turbines Under Blade Pitch System Fault, Grid Loss, and Shutdown Events," *Wind Energy* 17, no. 9 (2014): 1385–1409, https://doi.org/10.1002/we.1639.

52. C. Blary, F. Bonadonna, E. Dussauze, S. Potier, A. Besnard, and O. Duriez, "Detection of Wind Turbines Rotary Motion by Birds: A Matter of Speed and Contrast," *Conservation Science and Practice* 5 (2023): e13022, https://doi.org/10.1111/csp2.13022.

53. P. Enevoldsen and G. Xydis, "Examining the Trends of 35 Years Growth of Key Wind Turbine Components," *Energy for Sustainable Development* 50 (2019): 18–26, https://doi.org/10.1016/j.esd.2019.02.003.

54. C. D. Santos, H. Ramesh, R. Ferraz, A. M. A. Franco, and M. Wikelski, "Factors Influencing Wind Turbine Avoidance Behaviour of a Migrating Soaring Bird," *Scientific Reports* 12, no. 1 (2022): 6441, https://doi.org/10.1038/s41598-022-10295-9.

Supporting Information

Additional supporting information can be found online in the Supporting Information section.